

Study of scattering and fusion cross sections for $^{16}\text{O}+^{58,62}\text{Ni}$ around Coulomb barrier

Bidhubhusan Sahu,* Basudeb Sahu

Department of Physics, North Orissa University, Baripada-757003, INDIA

** email: bhusan3580@yahoo.co.in*

We investigate the measured results of elastic scattering and fusion cross sections of the $^{16}\text{O}+^{58,62}\text{Ni}$ systems at different incident centre of mass energy $E_{c.m.}$ around the Coulomb barrier. Both of these phenomena were explained simultaneously by adopting the convenient multistep potential approximation method [1]. The salient features of the above method are summarized below.

A smoothly varying potential $U(r)$ can be considered as a chain of 'n' number of rectangular potentials each one of which has arbitrarily small width 'w'. Having simulated the potential up to a maximum range $r=R_{max}$ we have $R_{max} = \sum_i^n w_i$

where $w_i = w$ is the width of the ith rectangle. Let

in the jth region, $\sum_{i=1}^{j-1} w_i < r \leq \sum_{i=1}^j w_i$, the strength and width of the potential be denoted by U_j and w_j respectively. Starting with the reduced Schrödinger equation in this region as,

$$\frac{d^2\Phi(r)}{dr^2} + \frac{2m}{\hbar^2}(E - U_j)\Phi(r) = 0 \quad (1)$$

with the solution

$$\Phi_j(r) = a_j e^{ik_j r} + b_j e^{-ik_j r}, \quad (2)$$

where the wave number k_j is defined as $k_j = \sqrt{2m/\hbar^2(E - U_j)}$ for the jth segment of width w_j and using the exact Coulomb wave function i.e. G_l and F_l and their derivatives in the outer region $r \geq R_{max}$ and the wave function $\Phi_n(r)$ and its derivative in the left side of $r = R_{max}$ we get the expression for partial wave S-matrix η_l as,

$$\eta_l = 2iC_l + 1 \quad (3)$$

$$\text{where } C_l = \frac{kF_l' - F_l H}{H(G_l + iF_l) - k(G_l' + iF_l')} \quad (4)$$

and $H = \Phi_n' / \Phi_n$. For the total reaction cross section one can use the formula

$$\sigma_r = \frac{\Pi}{k^2} \sum_l (2l+1)(1 - |\eta_l|^2) \quad (5)$$

This is equal to the absorption cross section

$$\sigma_{abs} = \frac{\Pi}{k^2} \sum_l (2l+1) \left(\sum_{j=1}^n I_j \right) \quad (6)$$

where I_j is the absorption cross section from the jth

region [1]. Using the expression (3) for η_l and the optical model potential parameters in Woods-Saxon form given in the table I, we calculate the result of elastic scattering cross section at energy $E_{LAB}=42$ MeV for $^{16}\text{O}+^{58,62}\text{Ni}$ systems and obtain a good explanation of the corresponding experimental data [2] as shown in figures 1 and 2.

TABLE I. Optical model potential parameters used in the calculations.

Parameters	$^{16}\text{O}+^{58}\text{Ni}$	$^{16}\text{O}+^{62}\text{Ni}$
V_N (MeV)	75.0	75.0
r_v (fm)	0.38	0.38
a_v (fm)	1.32	1.33
W (MeV)	3.0	3.0
r_w (fm)	1.3	1.3
a_w (fm)	0.15	0.15
r_c (fm)	1.2	1.2
V_B (MeV)	31.05	30.48
R_B (fm)	9.98	10.18
R_{fus} (fm)	7.3	7.4

With the same potential, the result of σ_{fus} and barrier

distribution as $D(E_{c.m.}) = \frac{d^2(E_{c.m.} \sigma_{fus})}{dE_{c.m.}^2}$ are

calculated and the corresponding experimental data [2, 3] (solid dots) in figures 3, 4 and 5 are explained with remarkable success by our calculated results shown by full curves. It is seen that good fits to data were obtained for both the systems, only with the use of little larger value $r_0=1.33$ fm and $R_f=7.4$ fm

for $^{16}\text{O}+^{62}\text{Ni}$. The weakly absorptive nature of the optical potential mentioned above is found to allow resonance states to occur in the collision of two nuclei. These resonances control the oscillatory or peak structures of $D(E_{c.m.})$ seen in figure 4 and 5. Further, such a weak absorption is sufficient because the real part is considered deep and less diffused to explain the elastic scattering cross section.

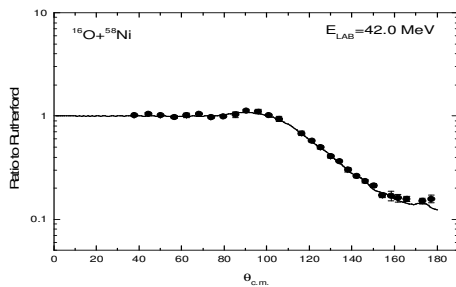


Fig. 1: Angular distribution of elastic scattering of $^{16}\text{O}+^{58}\text{Ni}$ at energy 42.0 MeV. The full drawn curve is our theoretical result. The experimental data shown by solid dots are obtained from [2].

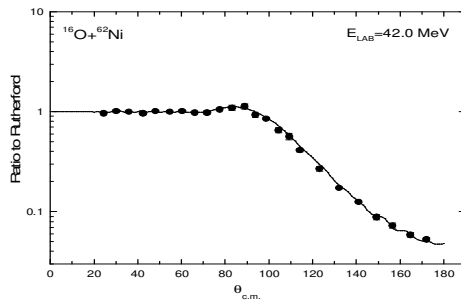


Fig. 2: Angular distribution of elastic scattering of $^{16}\text{O}+^{62}\text{Ni}$ at energy 42.0 MeV. The full drawn curve is our theoretical result. The experimental data shown by solid dots are obtained from [2].

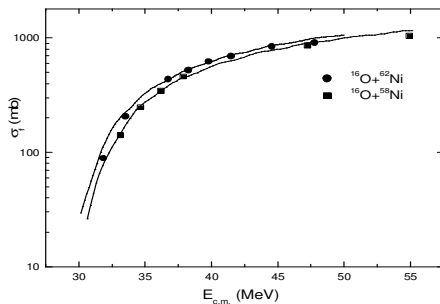


Fig. 3: Variation of σ_{fus} as function of $E_{c.m.}$ for $^{16}\text{O}+^{58,62}\text{Ni}$ systems. The full drawn curves represent

our calculated results. The experimental data shown by solid dots are obtained from [2].

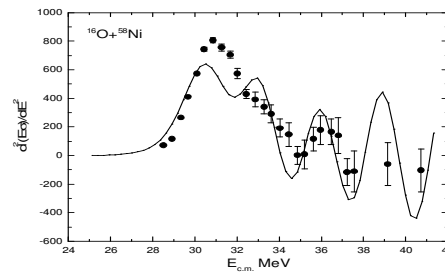


Fig. 4: Variation of $D(E_{c.m.})$ as function of energy $E_{c.m.}$ for $^{16}\text{O}+^{58}\text{Ni}$ corresponding to results of σ_{fus} in fig. 3. The experimental data shown by solid dots are obtained from [3].

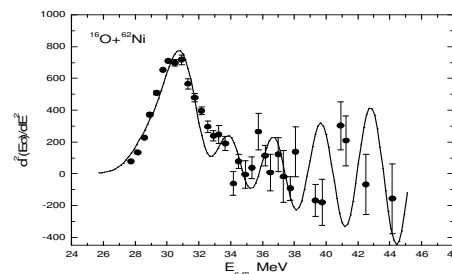


Fig. 5: Variation of $D(E_{c.m.})$ as function of energy $E_{c.m.}$ for $^{16}\text{O}+^{62}\text{Ni}$ corresponding to results of σ_{fus} in fig. 3. The experimental data shown by solid dots are obtained from [3].

This work is supported by DST, NEW Delhi, vi-de Grant No-SR/S2/HEP-18/2004

References

- [1] Basudeb Sahu et al., Phys Rev. C **77**, 024604 (2008)
- [2] N. Keely et al., Nucl. Phys. A **582** (1995) 314-334
- [3] N. Keely et al., Nucl. Phys. A **628** (1988) 1-16